STD NMR insights into interaction of monovalent mannose-based ligands with DC-SIGN

Anita Kotar[a,b], Tihomir Tomašič[b], Martina Lenarčič Živković[a], Gregor Jug[b], Janez Plavec[a,c,d*], Marko Anderluh[b,*]

[a]*Slovenian NMR center, National Institute of Chemistry, Hajdrihova 19, 1000 Ljubljana, Slovenia*

[b]*Faculty of Pharmacy, University of Ljubljana, Aškerčeva 7, 1000 Ljubljana, Slovenia*

[c]*EN-FIST Centre of Excellence, Trg OF 13, 1000 Ljubljana, Slovenia*

[d]*Faculty of Chemistry and Chemical Technology, University of Ljubljana, Aškerčeva 5, 1000 Ljubljana, Slovenia*

**Corresponding authors. Fax: Fax:+38614258031*, *E-mail:* marko.anderluh@ffa.uni-lj.si *(M. Anderluh), Fax: +38614760300, E-mail:* janez.plavec@ki.si *(J. Plavec)*

Table of contents:

Chemistry

NMR assignments and conformational properties of ligands

Fig. S1 ^{1}H NMR spectra of **1-4**.

Fig. S2 HSQC NMR spectrum of **2**.

Fig. S3 HSQC NMR spectrum of **3**.

Fig. S4 Structures of aryl moieties (R groups in Fig. 1) showing the atom numbering used in the NMR assignment.

STD build-up studies

Fig. S5 STD-amplification factor of **2** as a function of saturation time.

Fig. S6 STD-amplification factor of **3** as a function of saturation time.

Fig. S7 STD-amplification factor of **4** as a function of saturation time.

Evaluation of binding affinities

Fig. S8 The binding isotherm of STD-AF initial growth rates approach.

Molecular modelling

Fig. S9 Overlay of FlexX- and FRED-calculated binding modes of compounds (*R*)-3 and (*S*)-3.

Fig. S10 FRED docking poses of compounds 1 and 2.

Chemistry

General. Dichloromethane was dried over calcium hydride and *N,N*-dimethylformamide over activated molecular sieves. All reagents were used as received from commercial sources without further purification unless otherwise indicated. Analytical TLC was performed on Merck silica gel (60 F 254) plates (0.25 mm) and components visualized with staining reagents or ultraviolet light. Flash column chromatography was carried out on silica gel 60 (particle size 230-400 mesh). ^{1}H NMR and ^{13}C NMR spectra were recorded at 400 MHz and 100 MHz, respectively, on a Bruker AVANCE III spectrometer in DMSO-d_6 or CD_3OD solution, with TMS as internal standard at 25 °C. IR spectra were recorded on a Perkin-Elmer Spectrum BX FT-IR spectrometer. Mass spectra were obtained using a Autospec-Q VGAnalytical mass spectrometer. All reported yields refer to isolated purified products. Compounds **1** and **4** were synthesized as reported.[23, 25]

Methyl 3-hydroxybenzoate (6). A solution of 3-hydroxybenzoic acid (**5**) (3.365 g, 23.7 mmol) in MeOH (35 mL, dried over molecular sieves) was cooled on an ice bath to 0 °C and put under argon. Thionyl chloride (2.10 mL, 28.4 mmol) was then added drop wise. Reaction mixture was stirred at room temperature for 24 h, cooled and the solvent evaporated under reduced pressure. The oily residue was co-evaporated with diethyl ether (2 × 10 mL) to obtain compound **6** as a white amorphous solid. Yield: 3.591 g (99.8%); white amorphous solid; ^{1}H NMR (400 MHz, DMSO-d_6) δ 3.83 (s, 3H, CH_3), 7.04 (ddd, 1H, J_1 = 7.9 Hz, J_2 = 2.5 Hz, J_3 = 1.2 Hz, Ar-H), 7.32 (t, 1H, J = 7.9 Hz, Ar-H), 7.35 (dd, 1H, J_1 = 2.5 Hz, J_3 = 1.2 Hz, Ar-H), 7.39-7.41 (m, 1H, Ar-H), 9.84 (s, 1H, OH) ppm.

Methyl 3-(2-hydroxy-3-(naphthalen-1-yloxy)propoxy)benzoate (8). To a solution of **6** (3.316 g, 21.8 mmol) in methanol (25 mL) KOH (1.162 g, 20.7 mmol) was added. The reaction mixture was stirred at room temperature until KOH dissolved and then the solvent was evaporated under reduced pressure. The obtained potassium salt of **6** was dissolved in a mixture of toluene (40 mL) and *N,N*-dimethylformamide (10 mL) and **7** (4.38 g, 21.8 mmol) and tetrabutylammonium bromide (1.406 g, 4.36 mmol) were added. Reaction mixture was stirred at 90 °C for 24 h. The solvent was evaporated and the oily residue dissolved in ethyl acetate (100 mL). Organic phase was successively washed with water (2 × 30 mL), saturated aqueous $NaHCO_3$ solution (30 mL) and brine (30 mL), dried over Na_2SO_4, filtered and the solvent evaporated under reduced pressure. Crude product was purified by flash column chromatography using ethyl acetate/hexane (1:2) as eluent. Yield: 3.334 g (43.4%); yellow oil; ^{1}H NMR (400 MHz, DMSO-d_6) δ 3.84 (s, 3H, CH_3), 4.20-4.38 (m, 5H, CH, 2 × CH_2), 5.86 (d, 1H, J = 5.5 Hz, CHOH), 7.04 (d, 1H, J = 7.5 Hz, Ar-H), 7.30 (ddd, 1H, J_1 = 8.0 Hz, J_2 = 2.7 Hz, J_3 = 1.0 Hz, Ar-H), 7.39-7.57 (m, 5H, Ar-H), 7.86-7.88 (m, 2H, Ar-H), 8.18-8.27 (m, 2H, Ar-H) ppm.

Methyl 3-(2-(2,3,4,6-tetra-*O*-acetyl-α-D-mannopyranosyloxy)-3-(naphthalen-1-yloxy)propoxy)benzoate (9). To a solution of **8** (2.660 g, 7.55 mmol) and 2,3,4,6-tetra-*O*-acetyl-α-d-mannopyranosyl trichloroacetimidate (3.024 g, 6.29 mmol) in dry dichloromethane (70 mL) under argon trimethylsilyl trifluoromethanesulfonate (TMSOTf) (1.48 mL, 8.18

mmol) was added at 0°C. After stirring at 0°C for 30 min the reaction mixture was allowed to warm to room temperature and stirred overnight. Then Et_3N (2.3 mL, 16.4 mmol) was added and the reaction mixture was successively by washed with saturated aqueous $NaHCO_3$ solution (30 mL), water (30 mL) and brine (30 mL), dried over Na_2SO_4, filtered and the solvent evaporated under reduced pressure. Crude product was purified by flash column chromatography using ethyl acetate/hexane (1:2) as eluent. Compound **9** was obtained as a mixture of two diastereomers. Yield: 3.586 g (83.5%); yellow oil; ^{1}H NMR (400 MHz, DMSO-d_6) δ 1.89, 1.92 (2 × s, 3H, $OCOCH_3$), 1.93, 1.95 (2 × s, 3H, $OCOCH_3$), 1.98, 2.03 (2 × s, 3H, $OCOCH_3$), 2.12, 2.13 (2 × s, 3H, $OCOCH_3$), 3.85, 3.86 (2 × s, 3H, $COOCH_3$), 3.89-3.93 (m, 1H, mannose-H), 3.97-4.02 (m, 1H, mannose-H), 4.14-4.19 (m, 1H, mannose-H), 4.39-4.52 (m, 4H, $C\underline{H_2}CHC\underline{H_2}$), 4.54-4.61 (m, 1H, $CH_2C\underline{H}CH_2$), 5.08-5.21 (m, 3H, 3 × mannose-H), 5.37-5.39 (m, 1H, mannose-H), 7.05-7.11 (dd, 1H, J_1 = 14.4 Hz, J_2 = 7.7 Hz, Ar-H), 7.32-7.35 (m, 1H, Ar-H), 7.42-7.61 (m, 7H, Ar-H), 7.87-7.91 (m, 1H, Ar-H), 8.14-8.21 (m, 1H, Ar-H) ppm.

Methyl 3-(2-(α-D-mannopyranosyloxy)-3-(naphthalen-1-yloxy)propoxy)benzoate (3). Compound **9** (3.356 g, 4.92 mmol) was dissolved in dry methanol (50 mL) and sodium methanolate solution (30 wt. % in methanol, 0.30 mL, 1.60 mmol) was added. The reaction mixture was stirred at room temperature for 1 h and then the acidic ion exchange resin Amberlite® IR120 H was added for neutralization. After stirring of mixture for 10 min, the resin was filtered off, washed with methanol and the solvent removed *in vacuo*. Crude product was purified by flash column chromatography using chloroform/methanol (9:1) as eluent. Yield: 1.098 g (43.4%); white amorphous solid; IR (KBr) ν 3422, 2934, 1725, 1581, 1509, 1490, 1446, 1399, 1293, 1271, 1241, 1221, 1138, 1104, 1060, 1021, 974, 876, 794, 773, 756, 683, 572 cm^{-1}; ^{1}H NMR (400 MHz, DMSO-d_6) δ 3.41-3.54 (m, 3H), 3.60-3.69 (m, 3H), 3.84 (s, 3H, CH_3), 4.35-4.48 (m, 4H), 4.49-4.56 (m, 2H), 4.61 (dd, 1H, J_1 = 5.8 Hz, J_2 = 4.3 Hz, mannose-H), 4.76 (dd, 1H, J_1 = 9.2 Hz, J_2 = 5.2 Hz, mannose-H), 4.81 (t, 1H, J = 4.3 Hz, mannose-H), 5.05 (2 × d, 1H, J = 1.5 Hz, mannose-H-1), 7.05 (ddd, 1H, J_1 = 7.5 Hz, J_2 = 4.3 Hz, J_3 = 0.7 Hz, Ar-H), 7.31-7.34 (m, 1H, Ar-H), 7.40-7.58 (m, 7H, Ar-H), 7.86-7.90 (m, 1H, Ar-H), 8.16-8.24 (m, 1H, Ar-H) ppm; HRMS (ESI+): *m/z* for $C_{27}H_{31}O_{10}$ ($[M+H]^+$): calcd 515.1917; found 515.1911.

3-(2-(α-D-Mannopyranosyloxy)-3-(naphthalen-1-yloxy)propoxy)benzoic acid (2). Compound **3** (0.984 g, 1.91 mmol) was dissolved in ethanol (50 mL) and 1 M NaOH (11.5 mL, 11.5 mmol) was added. Reaction mixture was stirred at room temperature for 24 h and concentrated *in vacuo*. The obtained solution was acidified to pH = 2 using the 1 M HCl and the precipitate filtered off. Compound **2** was obtained as a white amorphous solid. Yield: 0.522 g (54.6%); white amorphous solid; IR (KBr) ν 3421, 2930, 1700, 1582, 1448, 1397, 1268, 1240, 1103, 1054, 1022, 978, 793, 771, 580, 571 cm^{-1}; ^{1}H NMR (400 MHz, CD_3OD) δ 3.68-3.91 (m, 6H, 6 × mannose-H), 4.39-4.51 (m, 4H, $C\underline{H_2}CHC\underline{H_2}$), 4.64-4.69 (m, 1H, $CH_2C\underline{H}CH_2$), 5.29 (d, 1H, J = 1.7 Hz, mannose-H-1), 6.99 (dd, 1H, J_1 = 7.5 Hz, J_2 = 1.0 Hz, Ar-H), 7.26 (ddd, 1H, J_1 = 8.3 Hz, J_2 = 2.6 Hz, J_3 = 1.0 Hz, Ar-H), 7.38-7.50 (m, 5H, Ar-H), 7.64-7.66 (m, 2H, Ar-H), 7.80-7.83 (m, 1H, Ar-H), 8.23-8.26 (m, 1H, Ar-H) ppm; HRMS (ESI-): *m/z* for $C_{26}H_{27}O_{10}$ ($[M+H]^+$): calcd 499.1604; found 499.1598.

NMR assignments and conformational properties of ligands

^{1}H and ^{13}C spectra were acquired on an Agilent Technologies DD2 600 MHz NMR spectrometer at 25 °C using 5 mm ^{1}H ($^{13}C/^{15}N$) ^{13}C enhanced Cold Probe. Data acquisition and processing was performed with software VNMRJ 3.2 version. Spectra for assignation were recorded in $^{2}H_2O$, 25 mM d_{11}-TRIS, 150 mM NaCl, 4 mM $CaCl_2$ for **1** and in DMSO-d_6 for **2-4** at 25 °C. Chemical shifts were referenced to the residual solvent signal of $^{2}H_2O$ at δ 4.8 ppm for **1** and of DMSO-d_6 at δ 2.5 ppm for ^{1}H (599.67 MHz) and δ 39.5 ppm for ^{13}C (150.80 MHz) for **2-4**.

Initially, 1D and 2D NMR spectra of **1-4** were acquired to evaluate their structural and conformational properties. Spectra were recorded in $^{2}H_2O$ for **1** and in DMSO-d_6 for **2-4** at 25 °C. The ^{1}H and ^{13}C NMR resonances of **1-4** have been assigned based on characteristic chemical shifts and signal multiplicity of 1D proton and carbon spectra, ^{1}H-^{1}H correlations in 2D COSY, TOCSY and NOESY spectra and ^{13}C-^{1}H correlations in 2D HSQC and HMBC spectra (for chemical shifts see the Experimental section). NMR assignments were in accordance with ligands' structures composed of α-D mannose and different aryl moieties connected by glycerol linker. For all four ligands the signals in the range between δ 3.3 and 3.9 ppm were assigned to hydrogens of sugar moieties. Anomeric proton is deshielded and appears at ca. δ 5.1 ppm. The major differences between ligands' spectra were detected in the region between δ 6.8 and 8.4 ppm, which is characteristic for aromatic protons. While the chirality of mannose moiety in **1-4** is invariant, there is an additional asymmetric centre in **1**, **2** and **3**, which leads to duplication of signals due to the presence of two diastereoisomers (Fig. S1). On the other hand, **4** showed a single set of resonances for mannose sugar due to the symmetric disposition of substituents on glycerol linker. The duplication of signals assigned to the naphthalene rings in **4** indicated that internal rotations were hindered.

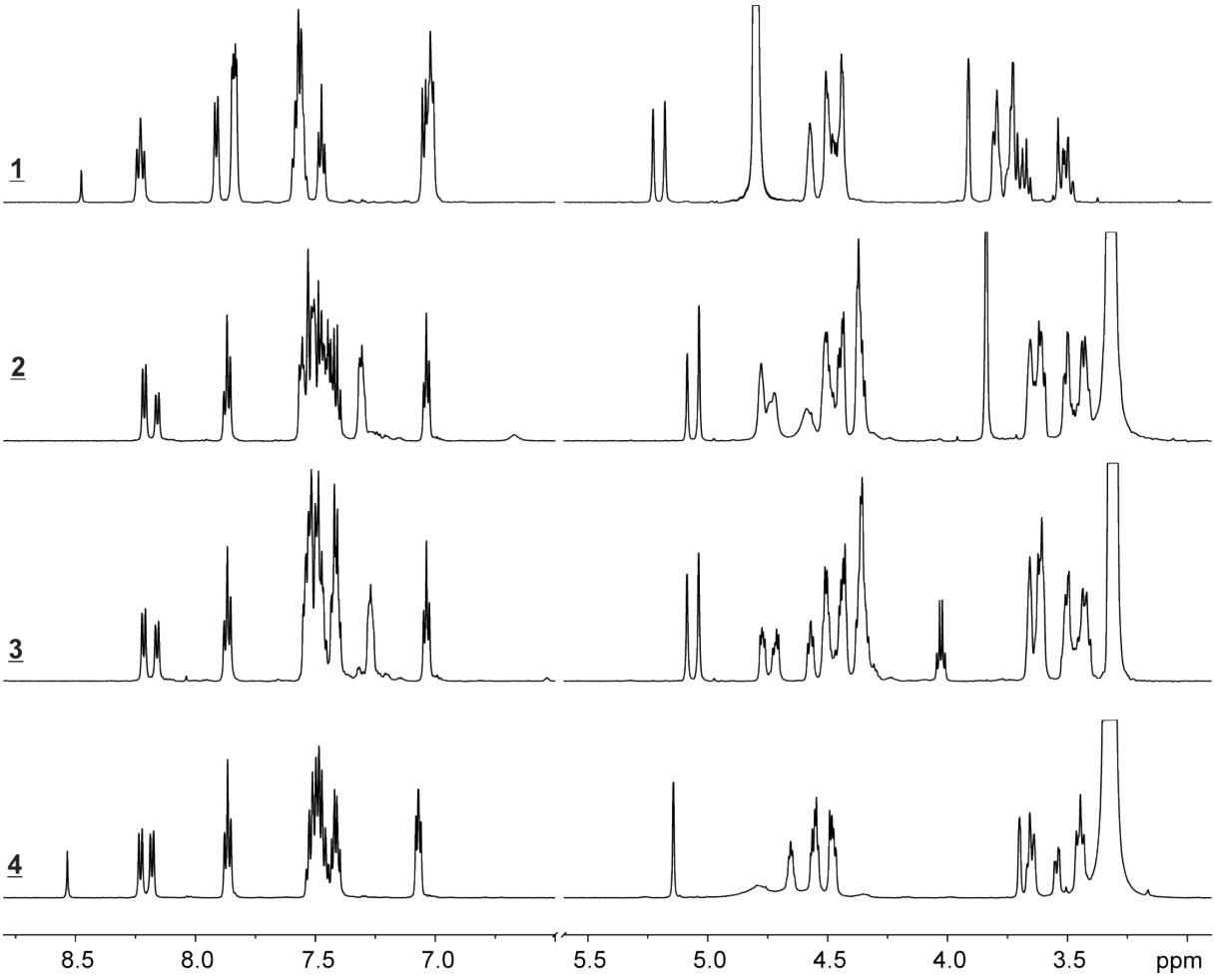

Fig. S1 1D ^{1}H NMR spectra of ligands **1-4**. The numbers of individual ligands are indicated on the left. Spectra were recorded at 600 MHz spectrometer in $^{2}H_2O$ for **1** and in DMSO-d_6 for **2-4** at 298 K.

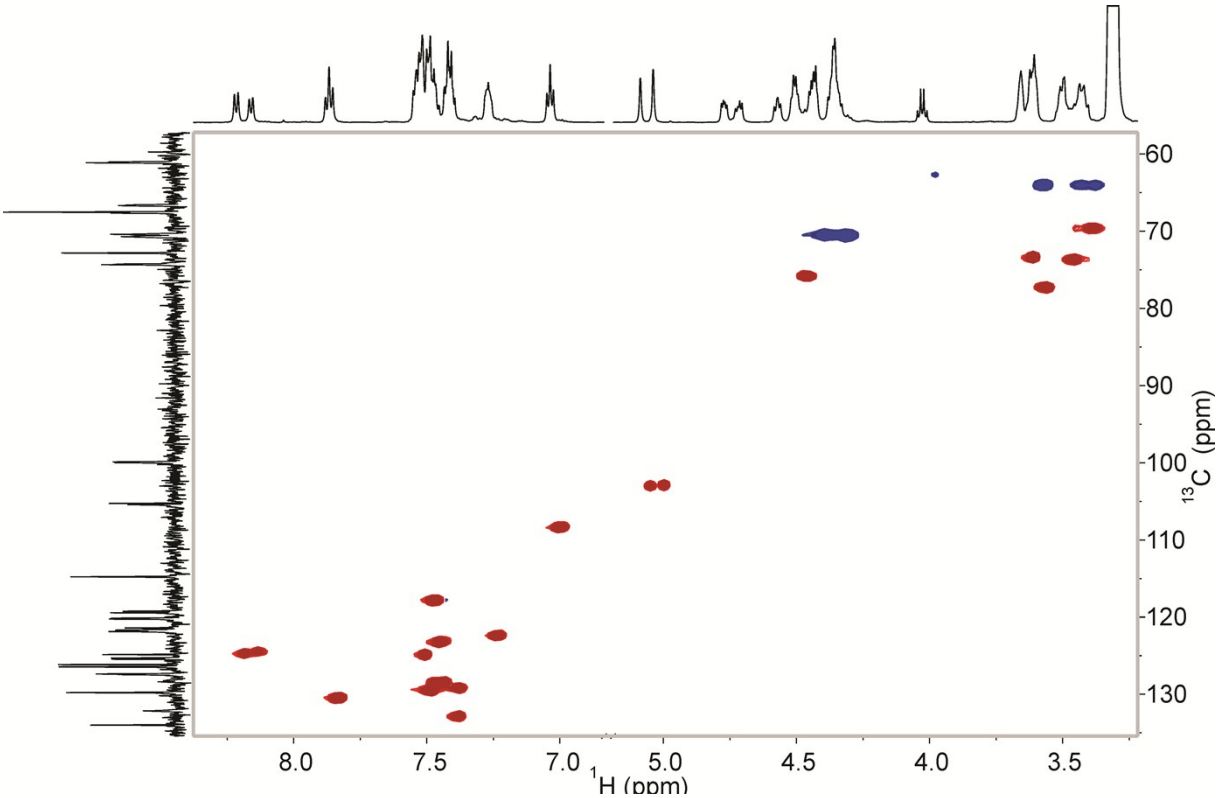

Fig.S2 HSQC NMR spectrum of **2** with ^{1}H NMR spectrum on x axis and ^{13}C NMR spectrum on y axis. Spectra were recorded at 600 MHz spectrometer in DMSO-d_6 at 298 K.

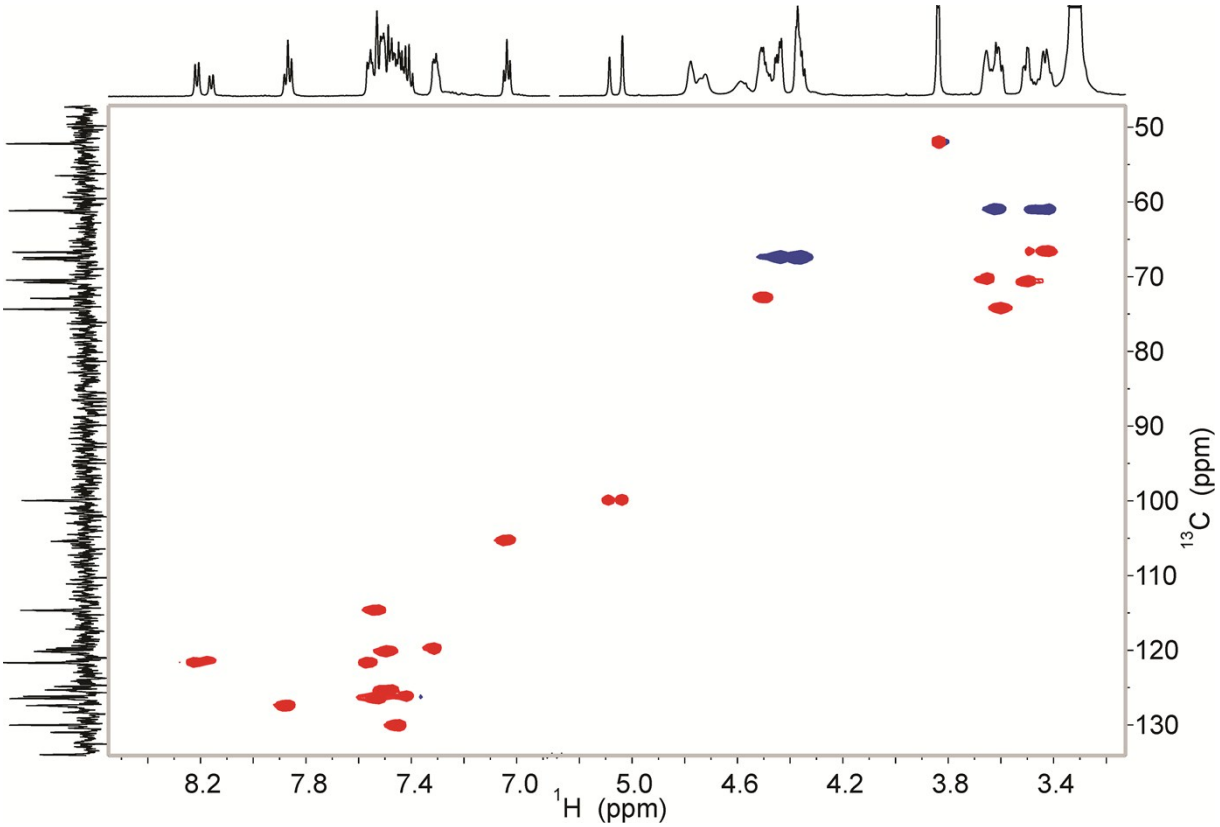

Fig. S3 HSQC NMR spectrum of d **3** with ^{1}H NMR spectrum on the x axis and ^{13}C NMR spectrum on the y axis. Spectra were recorded at 600 MHz spectrometer in DMSO-d_6 at 298 K.

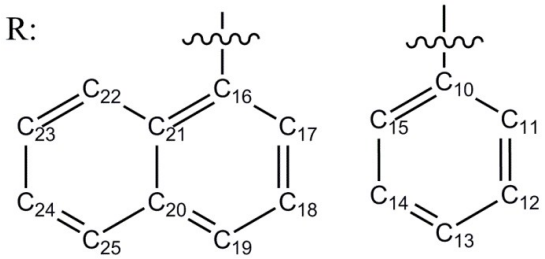

Fig. S4 Structures of aryl moieties (R groups in Fig. 1) showing the atom numbering used in the NMR assignment.

4-(2-(α-D-mannopyranosyloxy)-3-(naphthalen-1-yloxy)-propoxy)benzoic acid (1). ^{1}H NMR (600 MHz, $^{2}H_2O$), δ 3.47-3.54 (m, 2H, H-6, CH), 3.66-3.81 (m, 4H, H-3, H-4, H-5, H-6'), 3.91 (s, 1H, H-2), 5.18 and 5.23 (s, 1H, H-1), 4.44-4.51 (m, 4H, CH_2CHCH_2), 4.58 (m, 1H, CH_2CHCH_2), 7.01-7.05 (m, 3H, H-11, H-15, H-17), 7.47 (m, 1H, H-18), 7.54-7.60 (m, 3H, H-19, H-23, H-24), 7.84 (dd, 2H, J_1=8.4 Hz, J_2=3.3 Hz, H-12, H-14), 7.91 (d, 1H, J_1=8.4 Hz, H-25), 8.22 (d, 1H, J_1=9.6 Hz, H-22), 8.24 (d, 1H, J_1=9 Hz, H-22*) ppm; ^{13}C NMR (150 MHz, $^{2}H_2O$), δ 62.9, 63.2 (C-6), 68.9, 69.0 (C-4), 69.9, 70.40 (2x CH_2), 72.8, 72.83 (C-2), 72.9, 73.0 (C-3), 75.6, 75.7 (C-5), 76, 77.0 (CH), 102.3, 102.4 (C-1), 108.7, 109.1 (C-17), 116.8, 116.9 (C-11, C-15), 123.5, 123.7 (C-23), 123.9, 124.0 (C-22), 127.6 (C-21), 128.4, 128.5 (C-19), 128.9 (C-18), 129.5 (C-24), 130.26, 130.3 (C-25), 131.9 (C-13), 133.5, 133.6 (C-12, C-14), 136.9 (C-20), 156.2, 156.5 (C-16), 163.0, 163.2 (C-10), 177.7 (CO) ppm.

3-(2-(α-D-Mannopyranosyloxy)-3-(naphthalen-1-yloxy)propoxy)benzoic acid (2). ^{1}H NMR (600 MHz, DMSO-d_6), δ 3.41-3.51 (m, 3H, H-3, H-4, H-6), 3.61-3.66 (m, 3H, H-2, H-5, H-6'), 4.33-4.45 (m, 4H, CH_2CHCH_2), 4.50-4.51 (m, 1H, CH_2CHCH_2), 5.04 and 5.07 (s, 1H, H-1), 7.03 (d, 1H, J_1=7.2 Hz, H-17), 7.04 (d, 1H, J_1=7.2 Hz, H-17*), 7.26-7.28 (m, 1H, H-15), 7.40-7.44 (m, 2H, H-14, H-18), 7.46-7.55 (m, 5H, H-11, H-13, H-19, H-23, H-24), 7.86 (d, 1H, J_1=8.1 Hz, H-25), 7.87 (d, 1H, J_1=8.1 Hz, H-25*), 8.16 (d, 1H, J_1=8.0 Hz, H-22), 8.22 (d, 1H, J_1=8.2 Hz, H-22*) ppm; ^{13}C NMR (150 MHz, DMSO-d_6), δ 61.0, 61.2 (C-6), 66.7 (C-4), 67.5, 67.7 (2x CH_2), 70.4 (C-2), 70.7 (C-3), 72.8, 72.9 (CH), 74.3, 74.4 (C-5), 99.9, 100.0 (C-1), 105.4, 105.7 (C-17), 114.8, 114.82 (C-13), 119.2, 119.5 (C-15), 120.2, 120.3 (C-19), 121.4, 121.7 (C-22), 121.8, 121.9 (C-11), 124.9 (C-21), 125.3, 125.5 (C-23), 126.2 (C-18), 126.4, 126.5 (C-24), 127.4, 127.5 (C-25), 129.7, 129.8 (C-14), 132.8 (C-12), 133.9, 134.0 (C-20), 153.7, 153.8 (C-16), 158.3, 158.5 (C-10), 167.0 (CO) ppm.

Methyl 3-(2-(α-D-mannopyranosyloxy)-3-(naphthalen-1-yloxy)propoxy)benzoate (3). ^{1}H NMR (600 MHz, DMSO-d_6), δ 3.43-3.51 (m, 3H, H-3, H-4, H-6), 3.59-3.66 (m, 3H, H-2, H-5, H-6'), 3.84 (s, 1H, Me), 4.34-4.45 (m, 4H, CH_2CHCH_2), 4.48-4.51 (m, 1H, CH_2CHCH_2), 5.04 and 5.09 (s, 1H, H-1), 7.03 (d, 1H, J_1=7.2 Hz, H-17), 7.05 (d, 1H, J_1=7.2, H-17*), 7.30-7.32 (m, 1H, H-15), 7.40-7.57 (m, 7H, H-11, H-13, H-14, H-18, H-19, H-23, H-24), 7.86 (d, 1H, J_1=7.9 Hz, H-25), 7.88 (d, 1H, J_1=7.9 Hz, H-25*), 8.16 (d, 1H, J_1=8.1 Hz, H-22), 8.21 (d, 1H, J_1=8.3 Hz, H-22*) ppm; ^{13}C NMR (150 MHz, DMSO-d_6), δ 52.2 (Me), 61.2 (C-6), 66.8 (C-4), 67.5, 67.7 (2x CH_2), 70.4, 70.5 (C-2), 70.75, 70.8 (C-3), 73.0 (CH), 74.3, 74.4 (C-5), 99.9, 100.0 (C-1), 105.3, 105.5 (C-17), 114.6, 114.7 (C-11), 119.7, 119.9 (C-15), 120.2, 120.3 (C-19), 121.4 (C-22), 121.7 (C-13), 124.9 (C-21), 125.3, 125.5 (C-23), 126.2 (C-18), 126.4, 126.5 (C-24), 127.4 (C-25), 130.0 (C-14), 131.0 (C-12), 134.0 (C-20), 153.7 (C-16), 158.5 (C-10), 166.0 (CO) ppm.

1,3-Bis(naphthalen-1-yloxy)propan-2-yl α-D-mannopyranoside (4). ^{1}H NMR (600 MHz, DMSO-d_6), δ 3.43-3.46 (m, 2H, H-4, H-6), 3.53-3.55 (m, 2H, H-5, H-6'), 3.63-3.67 (dd, 1H, J_1=9 Hz, J_2=3 Hz, H-3), 3.70 (m, 1H, H-2), , 4.47-4.57 (m, 4H, CH_2CHCH_2), 4.65 (m, 1H, CH_2CHCH_2), 7.07 (m, 2H, H-17, H-17'), 5.14 (s, 1H, H-1), 7.40-7.54 (m, 8H, H-18, H-18', H-19, H-19', H-23, H-23', H-24, H-24'), 7.86 (d, 1H, J_1=7.8 Hz, H-25), 7.87 (d, 1H, J_1=8.4 Hz, H-25'), 8.18 (d, 1H, J_1=7.8 Hz, H-22), 8.23 (d, 1H, J_1 =8.4 Hz, H-22') ppm; ^{13}C NMR (150 MHz, DMSO-d_6), δ 61.2 (C-6), 66.8 (C-4), 67.6, 67.7 (2x CH_2), 70.5 (C-2), 70.8 (C-3), 73.1 (CH), 74.5 (C-5), 100.1 (C-1), 105.3, 105.5 (C-17), 120.2, 120.3 (C-19), 121.4, 121.7 (C-22), 124.8, 124.9 (C-21), 125.5 (C-23), 126.2 (C-18), 126.4, 126.5 (C-24), 127.4, 127.5 (C-25), 134.0 (C-20), 153.8, 153.9 (C-16) ppm.

STD build-up studies

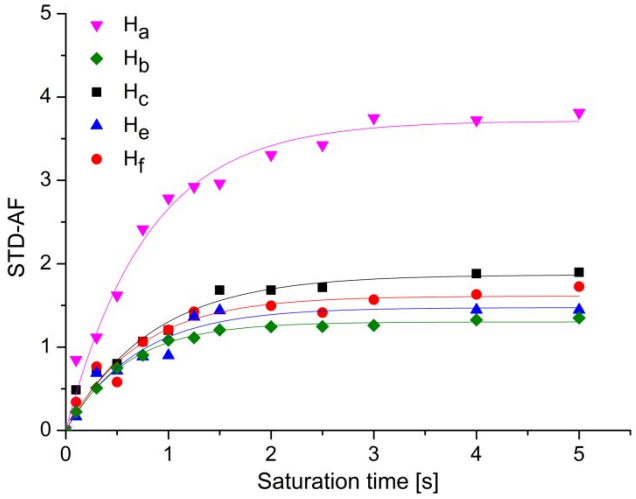

Fig. S5 STD-amplification factor of **2** as a function of saturation time. Experimental data were fitted to a rising exponential Eq. 2 to obtain the STD_{max} and k_{sat}. Symbols represent data, whereas solids lines are the mathematical least-square fits. (H_a: STD_{max}=3.71 ± 0.09, k_{sat}=1.26 ± 0.10 s^{-1}, R^2=0.982; H_b: STD_{max}=1.30 ± 0.01, k_{sat}=1.66 ± 0.06 s^{-1}, R^2=0.996, H_c: STD_{max}=1.87 ± 0.07, k_{sat}=1.20 ± 0.14 s^{-1}, R^2=0.948; H_e: STD_{max}=1.48 ± 0.08, k_{sat}=1.43 ± 0.23 s^{-1}, R^2=0.956; H_f: STD_{max}=1.61 ± 0.07, k_{sat}=1.41 ± 0.20 s^{-1}, R^2=0.948)

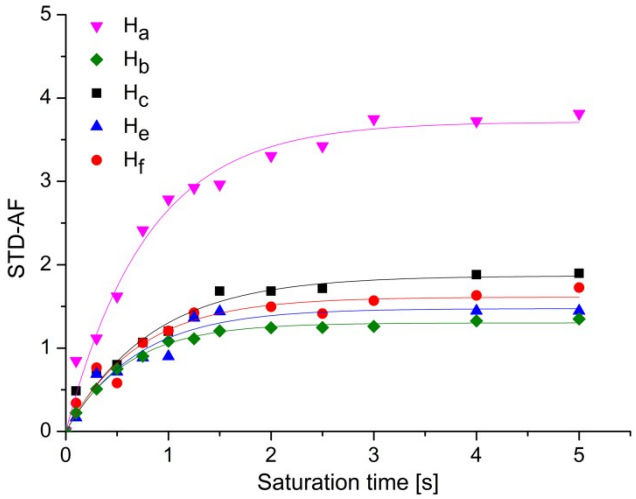

Fig. S6 STD-amplification factor of **3** as a function of saturation time. Experimental data were fitted to a rising exponential Eq. 2 to obtain the STD_{max} and k_{sat}. Symbols represent data, whereas solids lines are the mathematical least-square fits. (H_a: STD_{max}=3.44 ± 0.05, k_{sat}=1.19 ± 0.08 s^{-1}, R^2=0.993; H_b: STD_{max}=2.01 ± 0.09, k_{sat}=1.21 ± 0.05 s^{-1}, R^2=0.986, H_c: STD_{max}=1.58 ± 0.03, k_{sat}=1.38 ± 0.09 s^{-1}, R^2=0.990; H_e: STD_{max}=1.08 ± 0.02, k_{sat}=2.45 ± 0.03 s^{-1}, R^2=0.973; H_f: STD_{max}=1.77 ± 0.02, k_{sat}=1.35 ± 0.15 s^{-1}, R^2=0.969)

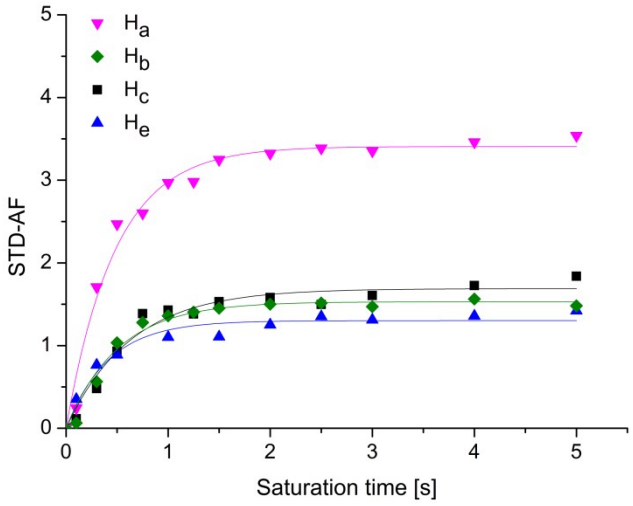

Fig. S7 STD-amplification factor of **4** as a function of saturation time. Experimental data were fitted to a rising exponential Eq. 2 to obtain the STD_{max} and k_{sat}. Symbols represent data, whereas solids lines are the mathematical least-square fits. (H_a: STD_{max}=3.41 ± 0.07, k_{sat}=2.08 ± 0.18 s^{-1}, R^2=0.980; H_b: STD_{max}=1.53 ± 0.04, k_{sat}=1.97 ± 0.20 s^{-1}, R^2=0.976, H_c: STD_{max}=1.69 ± 0.06, k_{sat}=1.59 ± 0.20 s^{-1}, R^2=0.962; H_e: STD_{max}=1.30 ± 0.04, k_{sat}=2.44 ± 0.32 s^{-1}, R^2=0.964)

Evaluation of binding affinities

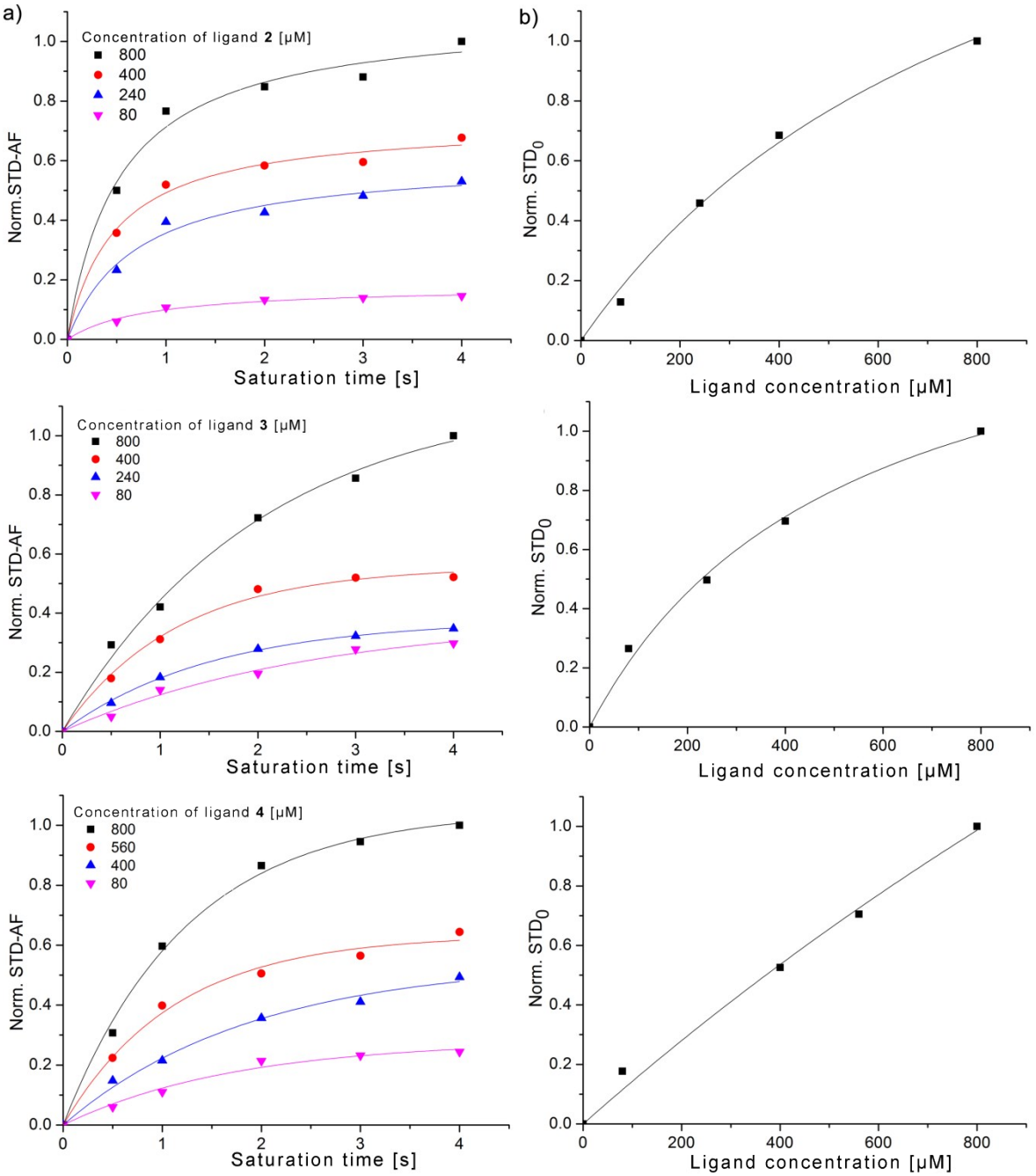

Fig. S8 The binding isotherm of STD-AF initial growth rates approach. a) Normalised STD-amplification factors of **2** (top), **3** (middle) and **4** (bottom) as a functions of saturation times for concentrations from 80 to 800 μM. The STD-AF values were obtained at different saturation times (1.0-4.0 s) and fitted to Eq. 2. b) Initial slopes of normalized STD_0 of **2** (top), **3** (middle) and **4** (bottom) as a function of ligand concentration. The experimental data were fitted to Eq. 3. The obtained K_D values were 0.9 mM, for **2**, 0.51 mM for **3** and 3.0 mM for **4**.

Molecular modelling

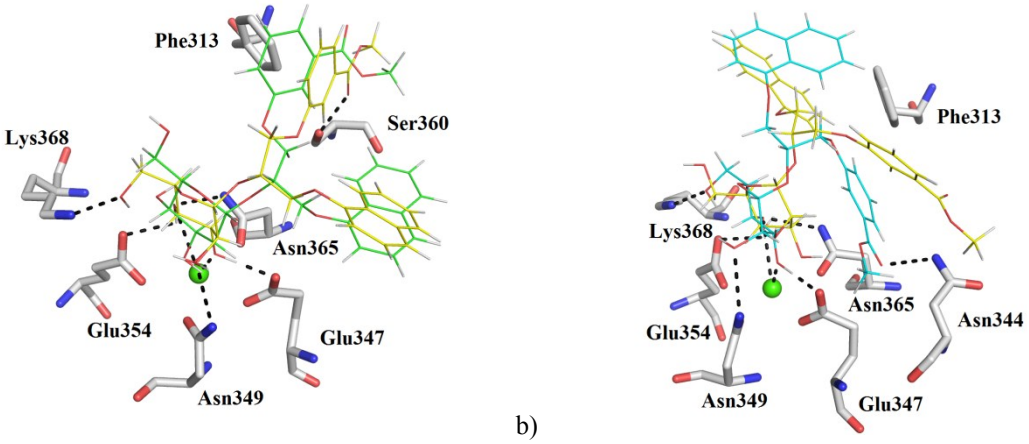

a) b)

Fig. S9 Overlay of docking poses of compounds a) (***R***)**-3** (FlexX pose in *yellow lines*, FRED pose in *green lines*) and b) (***S***)**-3** (FlexX pose in *cyan lines*, FRED pose in *yellow lines*) in DC-SIGN CRD Ca^{2+}-binding site. For clarity only side chains of amino acid residues predicted to interact with the docked ligands are shown as *grey sticks*. Ca^{2+} ion is presented as a *green sphere*. Hydrogen bonds for FlexX-docking pose are shown as *black dashed lines*. Figure was prepared by PyMOL.

a)

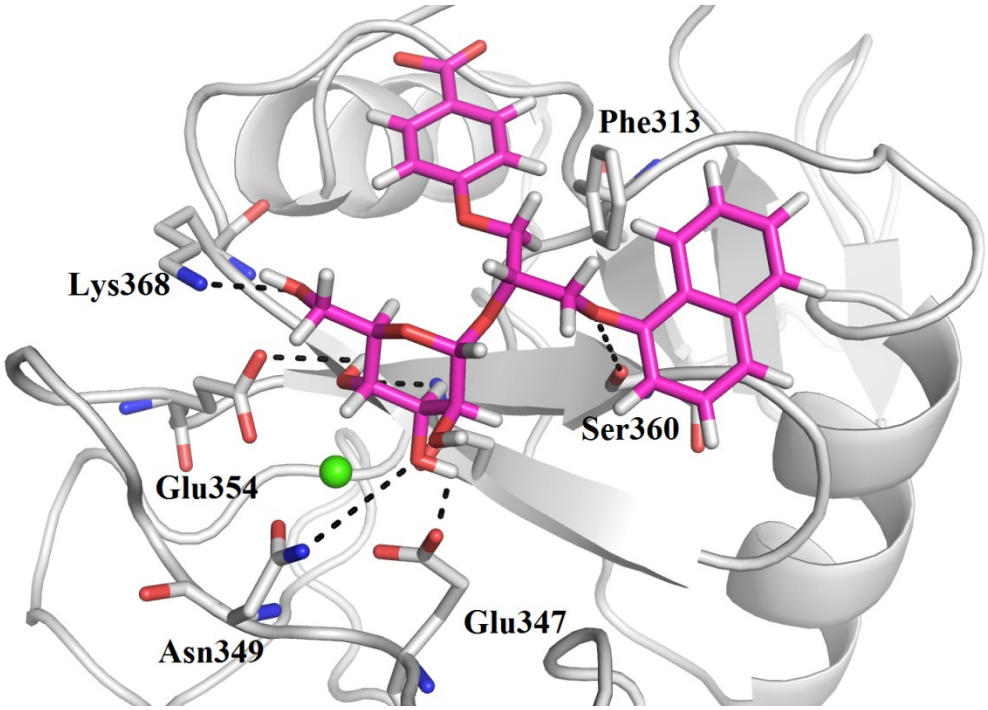

b)

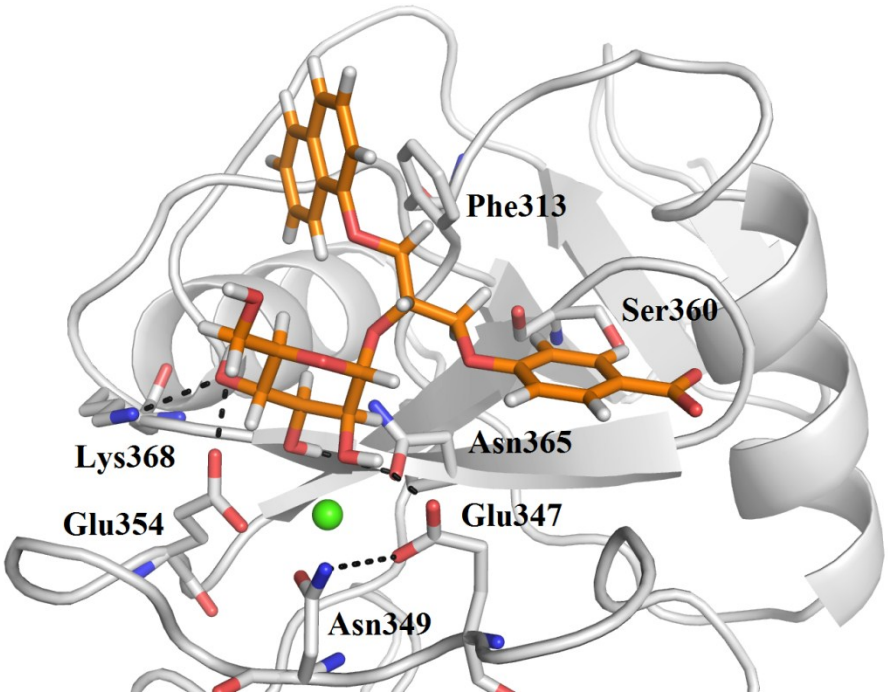
Phe313
Ser360
Lys368
Asn365
Glu354
Glu347
Asn349

c)

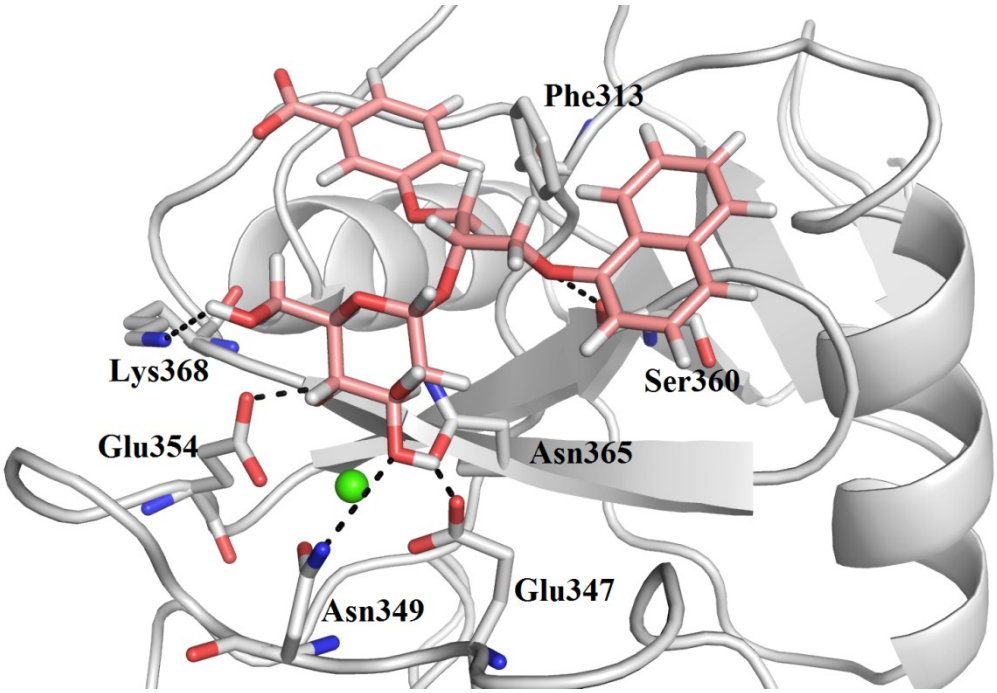
Phe313
Lys368
Ser360
Glu354
Asn365
Glu347
Asn349

d)

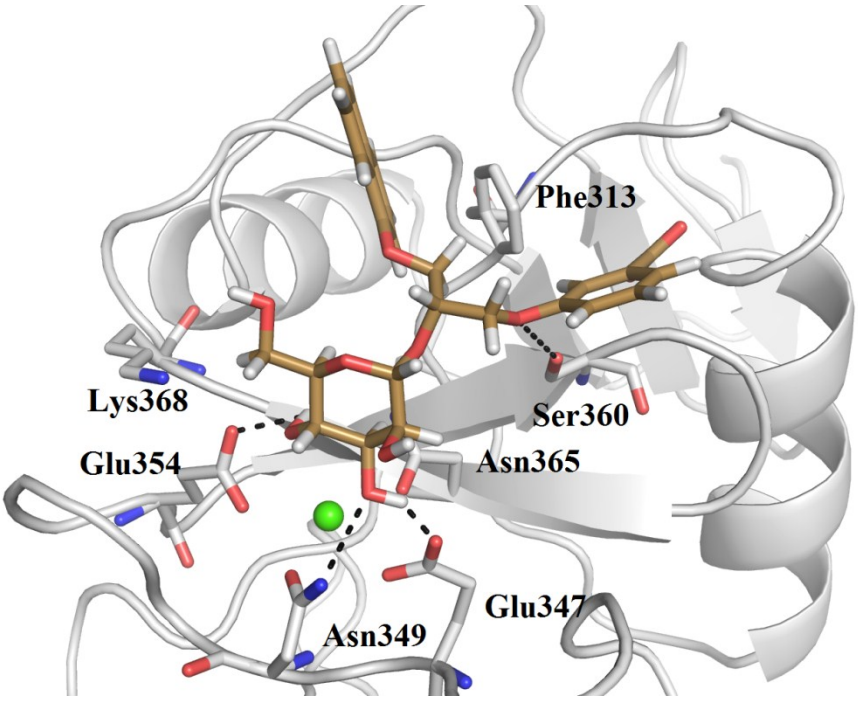

Fig. S10 FRED docking poses of compounds a) (***R***)-**1** (in *magenta sticks*), b) (***S***)-**1** (in *orange sticks*), c) (***R***)-**2** (in *pink sticks*) and d) (***S***)-**2** (in *brown sticks*) in DC-SIGN CRD Ca^{2+}-binding site. Protein (PDB entry: 1SL4) is presented in *grey cartoon* and Ca^{2+} ion as a *green sphere*. For clarity only side chains of amino acid residues predicted to interact with the docked ligands are shown as *grey sticks*. Hydrogen bonds are shown as *black dashed lines*. Figure was prepared by PyMOL.